Microstructural modification of cast aluminum alloys via friction stir processing

Z.Y. Ma*, S. R. Sharma*, R.S. Mishra*, and M.W. Mahoney**

*Department of Metallurgical Engineering, University of Missouri, Rolla, MO 65401, USA

** Rockwell Scientific, 1049 Camino Dos Rios, Thousand Oaks, CA 91360, USA

Keywords: friction stir processing, microstructural modification, cast aluminum alloy, A356

Abstract. Friction stir processing (FSP) is a new solid state processing technique for microstructural modification in metallic materials. FSP has been applied to cast aluminum alloy A356 plates to modify the microstructure to enhance mechanical properties. FSP broke up and dispersed the coarse acicular Si particles creating a uniform distribution of Si particles in the aluminum matrix. Further, FSP healed the casting porosity. These microstructural changes led to a significant improvement in both strength and ductility. Generally, high tool rotation rate is beneficial to break coarse Si particles, heal the casting porosity, and consequently increase strength. For a standard pin, maximum strength was achieved at a tool rotation rate of 900 rpm for a constant traverse speed of 8 ipm. A tri-flute pin design produced an optimum combination of strength and ductility compared to the standard and cone-shaped pins.

Introduction

Al-7wt.%Si-Mg alloys with Mg contents in the range of 0.25 to 0.65 wt% (A356 and A357 alloys) are widely used to cast high-strength components in the aerospace and automobile industries because they offer a combination of high achievable strength [1-3] with good casting characteristics [4]. However, the mechanical properties of cast alloys, in particular toughness and fatigue resistance, are limited by three drawbacks, i.e., porosity, coarse acicular Si particles, and coarse primary aluminum dendrites [5-8].

In the past two decades, various modification and heat-treatment techniques have been developed to refine the microstructure of cast Al-Si alloys. The first category of research is aimed at modifying the morphology of Si particles. Generally, chemical modification and thermal treatment have been adopted to modify the coarse acicular Si particles to fine and globular particles [8-10]. Chemical modification methods involve adding very small amounts of sodium, strontium, or antimony, known as eutectic modifiers [9,10]. Sodium is a good modifier and has been traditionally used to spheroidize eutectic particles. However, the benefits of sodium fade rapidly on holding at high temperature and the modifying action practically disappears after only two remelts. On the other hand, the modifying effect of strontium does not fade on holding at elevated temperature and its use has become more widespread. However, longer holding time is required at 750^{o}C due to the difficulty in dissolution of strontium, resulting in increased gas pickup [11]. Furthermore, microshrinkage porosity is also higher after the addition of strontium owing to the dissolution difficulty and a depression in the eutectic transformation temperature [12]. Finally, although antimony has no fading effect and the improvement in elongation and impact strength is greater than that achieved by sodium [9], its use has been precluded in most countries because of environmental and safety reasons. Thermal modification involves heat-treatment of cast alloys at high temperature, usually at the solid solution temperature around 540^{o}C for long times [8]. Solution heat treatment results in a substantial degree of spheroidization of Si particles and also coarsens Si particles. However, for large and complex cast aluminum components for engineering applications solution treatment is not practical.

The second research category refines the coarse primary aluminum phases. A heat treatment at an extremely high temperature of 577^{o}C for a short time of 8 min resulted in a substantial refinement in the aluminum dendrites in a semi-solid processed (SSP) A356. This heat treatment increases both yield and ultimate tensile strengths of A356 [3]. More recently, Wang et al. [13] reported that a melt thermal treatment led to remarkable refinement of the aluminum phase of A356, thereby resulting in a significant improvement in both strength and ductility.

None of the modification and heat-treatment techniques mentioned above can eliminate the porosity effectively in A356 and redistribute the Si particles uniformly into the aluminum matrix. Therefore, a more effective modification technique is highly desirable for microstructural modification of cast A356 to enhance mechanical properties, in particular, ductility and fatigue. Friction stir processing (FSP), a development based on friction stir welding (FSW) [14], is a new solid processing technique for microstructural modification [15,16]. The basic concept of FSP is remarkably simple. A rotating tool with pin and shoulder is inserted into a single piece of material and traversed along the desired path to cover the region of interest and thus modify the local microstructure. Friction between the tool and workpiece and severe plastic deformation results in localized heating that softens and plasticizes the workpiece. A volume of processed material with extensive mixing is produced by movement of material in a complex path around the pin. The characteristics of FSP have resulted in several applications for microstructural modification in metallic materials. First, FSP has been used to generate a fine-grained microstructure amenable to high strain rate superplasticity (HSRS) [15,17]. Second, FSP can be used to produce a surface composite on an aluminum substrate [18]. Third, FSP has been verified to be an effective approach to homogenize the microstructure of nanophase aluminum alloys [19].

In this study, FSP is adopted to modify the microstructure of unmodified cast A356 to enhance mechanical properties. Different processing parameters (tool rotation rate and traverse speed) and pins designs were used to evaluate the effects of FSP parameter and tool geometry on the microstructural changes and resultant mechanical properties.

Experimental

Commercial A356 cast plates with nominal composition 7.0Si-0.3Mg-bal Al (in wt. pct) were used for FSP. The billet was received in the as-cast condition. Single pass friction stir processing was performed on 12.7 mm thick A356 cast plates. Pin geometries and processing parameters used for FSP are summarized in Table 1. As-processed aluminum plates were cut transverse to the processing direction, mounted, and mechanically polished. Microstructural examination was completed with optical microscopy (OM). The size and aspect ratio of Si particles and the porosity level were analyzed by means of Scion Image software. All FSP samples were kept at room temperature for more than one month to naturally age after FSP. To evaluate the effect of FSP on the properties of cast A356, mini tensile specimens of 1.3 mm gage length and 1.0 mm gage width were electro-discharge machined in the transverse direction from the FSP region. These specimens were subsequently ground and polished to a final thickness of ~0.5 mm. Tensile tests were conducted at room temperature using a computer-controlled, custom-built mini tensile tester with a initial strain rate of 1×10^{-3} s^{-1}. For comparison, mini specimens of the as-received A356 were also tested using the same experimental conditions and specimen geometry. To understand the effect of post-process aging on the properties of FSP samples, samples were subjected to artificial aging (155^{o}C for 4h).

Results and Discussion

A. Microstructure

Figure 1a shows an optical micrograph of a polished A356 casting in the as-received condition. Coarse acicular Si particles were distributed along the primary aluminum dendrite boundaries. The average grain size was ~100 μm and the Si particles had an aspect ratio of up to 15. The microstructure shown in Fig.1a is typical of unmodified sand-cast A356. Furthermore, porosity of ~ 50 μm diameter was detected in the as-received A356 plates. Figures 1b-i shows optical micrographs of FSP A356 for various process parameters using different pins. FSP resulted in a significant breakup of acicular Si particles and subsequently a uniform redistribution in the aluminum matrix. Furthermore, porosity in the as-cast A356 was nearly eliminated by FSP. Table 2 summarizes the size and aspect ratio of Si particles and porosity level in both as-cast and FSP alloys. Because the Si particles frequently connect to each other in the as-cast alloy, this tends to overestimate the particle size and underestimate their aspect ratio by means of Scion Image software. Therefore, the size and aspect ratio of Si particles for the as-cast alloy is subject to error. Three important observations can be made from the data presented in Table 2. First, FSP resulted in significant decreases in the size and aspect ratio of Si particles and the porosity level. Second, increasing the tool rotation rate reduces the size and aspect ratio of the Si particles and porosity level except for the standard pin at 1100 rpm. Third, generally, the tri-flute pin was more effective in breaking up Si particles and eliminating porosity than the standard pin and the cone-shaped pin.

Different explanations have been proposed for the deformation process during FSW and FSP. Krishnan [20] and Reynolds et al. [21] suggested that FSW is likened to an extrusion process. During each rotation of the tool, a semicylindrical portion of the material is pushed to the back of the tool and around to the retreating side. A cross-sectional slice through such a set of semicylinders results in the onion ring structure that is often observed in traverse sections of the FSW/FSP nugget [20]. In this case, there is very little material mixing during the FSW process.Conversely, Biallas et al. [22] suggested that when the material flows around the pin within the plane of the sheet, it is reflected approximately at the imaginary walls of the groove that would be formed in the case of regular milling of the metal. The induced circular movement leads to circles that decrease in radii and form the tube system. In this case, it is believed that there should be thorough mixing of material in the nugget region.

The present results indicate that FSP cannot be simply considered as an extrusion process, particularly with the threaded pins used in this study. An extrusion process cannot significantly break up coarse acicular Si particles and aluminum dendrites and uniformly disperse the broken Si particles into aluminum matrix. Generally, higher tool rotation rate created more intense stirring and mixing of material and a higher temperature rise. Thus, the ability of the rotating tool to breakup coarse acicular Si particles and eliminate porosity increases with increasing tool rotation rate. The threaded pins result in a superimposed vertical and horizontal material flow from geometrical considerations. The threads tend to move material downward along the pin wall and once this material reaches the bottom, the geometrical constraints require that the material move up away from the pin wall. The lateral traverse of the pin requires that the material move from front to back. How these three material flow patterns, based on geometrical and volume constraints, interact with each other is complex. However, significant progress has been made to understand the complex flow patterns using marker studies coupled with computational modeling. [23] Based on these intuitive considerations, higher rpm and lower ipm would result in more material movement and thus more mixing.

B. Tensile Properties

Table 3 summarizes the room-temperature tensile properties of FSP and as-cast A356 samples under as-FSP and aged conditions. The as-received A356 casting exhibits an ultimate tensile strength of 169 MPa, a yield strength of 132 MPa, and an elongation of 3%. Aging at 155^{o}C for 4 h resulted in a slight increase in yield strength, but a decrease in ultimate tensile strength and ductility. FSP resulted in a significant improvement in tensile properties, particularly the ductility. The elongation-to-failure was improved by one order of magnitude after FSP. Clearly, the improvement in mechanical properties of FSP A356 can be attributed to the elimination of porosity, significant microstructural refinement, and homogenization.

Generally, increasing the tool rotation rate increases strength for all three pin geometries except for the standard pin at a rotation rate of 1100 rpm (Table 3). However, the ductility does not decrease except for the sample processed by the cone-shaped pin. This is partially attributed to the decrease in the size and aspect ratio of Si particles and reduction in the porosity level. Furthermore, the higher temperature produced at the higher tool rotation rate is likely to more efficiently dissolve the Mg_2Si precipitates into the aluminum matrix. Mg_2Si is the primary strengthening phase. After FSP, precipitation occurred during room-temperature natural aging, resulting in an increase in the strength of the FSP samples processed at higher tool rotation rates.

Table 3 shows that the effect of tool geometry on mechanical properties is synergistic with the FSP parameters. For example, at 300 rpm/ 2ipm, strengths for the standard and tri-flute pins are higher than the cone-shaped pin whereas at 700 rpm/ 8ipm, the cone-shaped and tri-fluted pins are more effective in increasing the strength of A356 than the standard pin.

Aging at 155^{o}C for 4 h resulted in an increase in strength, in particular yield strength for FSP A356 processed at higher tool rotation rates of 700 -1100 rpm. However, artificial aging did not affect the strength of FSP samples prepared at the lower rotation rate of 300 rpm. As mentioned above, a higher tool rotation rate resulted in dissolution of more precipitate into solution with subsequent re-precipitation during artificial aging, thereby increasing the strength of FSP A356 samples. For low rotation rates, less precipitates dissolved into the aluminum matrix. Consequently, artificial aging did not result in extensive reprecipitation and as a result, strength of the FSP samples was not increased.

The overall implication of the present results is significant. These results show the effectiveness of using a simple FSP technique to improve significantly the mechanical properties of cast Al-Si alloys. Research is under progress to evaluate the effect of FSP parameters and tool geometries on the mechanical properties of cast A356 by using full-size specimens. In addition, it is expected that a uniform and fine microstructure will improve other mechanical properties such as fatigue. Fatigue testing is part of our on-going effort to study the influence of FSP on properties.

Conclusions

1. Friction stir processing resulted in a significant breakup of coarse acicular Si particles and primary aluminum dendrites, created a homogeneous distribution of Si particles in the aluminum matrix, and nearly eliminated all casting porosity. These microstructural modifications significantly improved the tensile properties of cast A356, in particular ductility.
2. In general, the strength of FSP A356 increased with increasing tool rotation rates. For the standard pin, a maximum strength was observed at a tool rotation rate of 900 rpm.
3. Artificial aging at 155°C for 4 h increased both the yield and ultimate tensile strengths of FSP A356 processed at higher rotation rates of 700-1100 rpm. However, such an aging treatment did not affect the strength of FSP samples prepared at the lower rotation rate of 300 rpm.
4. The effect of tool geometry on mechanical properties is complicated, and depends on the FSP parameters. The tri-flute pin produced an optimum combination of strength and ductility.

Acknowledgement

The authors gratefully acknowledge the support of (a) the National Science Foundation through grant DMR-0076433 and the Missouri Research Board for the acquisition of a friction stir welding and processing machine and (b) DARPA for supporting this work under contract No. MDA972-02-C-0030.

References

1. D. L. Zhang and L. Zheng: Metall. Mater. Trans., Vol. 27A (1996), p. 3983.
2. T. Din and J. Campbell: Mater. Sci. Technol., Vol. 12 (1996), p. 644.
3. Y. B. Yu, P. Y. Song, S. S. Kim, J. H. Lee: Scripta Mater., Vol. 41 (1999), p. 767.
4. Aluminum Casting Technology, 2nd edition, Ed. By D. L. Zalensas, AFS Inc. Illinois, (1993), P. 77.
5. S. Kumai, J. Hu, Y. Higo, S. Nunomura: Acta Mater., Vol. 44 (1996) p. 2249.
6. B. Zhang, D. R. Poirier, W. Chen: Metall. Mater. Trans., Vol. 30 (1999) p. 2659.
7. M. E. Seniw, J. G. Conley, M. E. Fine: Mater. Sci. Eng., Vol. A285 (2000) p. 43.
8. G. Atxaga, A. Pelayo, A. M. Irisarri: Mater. Sci. Technol., Vol. 17 (2001) p. 446.
9. K. T. Kashyap, S. Murrall, K. S. Raman, and K. S. S. Murthy: Mater. Sci. Technol., Vol. 9 (1993) p. 189.
10. L. Wang and S. Shivkumar: Z. Metallkd., Vol. 86 (1995) p. 441.
11. T. J. Hurley and R. G. Atkinson: Trans. AFS, Vol. 91 (1985) p. 291.
12. D. Argo and J. E. Gruzleski: Trans. AFS, Vol. 16 (1988) p. 65.
13. J. Wang, S. He, B. Sun, K. Li, D. Shu, Y. Zhou, Mater. Sci. Eng., Vol. A338 (2002) p. 101.
14. W. M. Thomas, E. D. Nicholas, J. C. Needham, M. G. Murch, P. Templesmith, and C. J. Dawes, G. B. Patent Application No, 9125978.8, Dec. 1991.
15. R. S. Mishra, M. W. Mahoney, S. X. McFadden, N. A. Mara, and A. K. Mukherjee: Scripta Mater., Vol. 42 (2000) p. 163.
16. R. S. Mishra and M. W. Mahoney: Mater. Sci. Forum, Vol. 357-3 (2001) p. 507.
17. Z. Y. Ma, R. S. Mishra, M. W. Mahoney: Acta Mater., Vol. 50 (2002) p. 4419.

18. R. S. Mishra, Z. Y. Ma, I. Charit: Mater. Sci. Eng., Vol. 341A (2003) p. 307.

19. P. B. Berbon, W. H. Bingel, R. S. Mishra, C. C. Bampton, M. W. Mahoney: Scripta Mater., Vol. 44 (2001) p. 61.

20. K. N. Krishnan: Mater. Sci. Eng., Vol. A327 (2002) p. 246.

21. A. P. Reynolds, T. U. Seidel, M. Simonnen: First International Conference on Friction Stir Welds, Thousand Oaks, CA, USA, 1999.

22. G. Biallas, R. Braun, C. D. Donne, G. Staniek, W. A. Keysser: First International Conference on Friction Stir Welds, Thousand Oaks, CA, USA, 1999.

23. A. Askari, S. Sillling, B. London, and M. Mahoney, TMS Proceedings, Indianapolis, Indiana, Nov. 4-8, 2001,

Table 1. Summary of pin geometry and processing parameters for FSP A356.

Processing parameter	Tool geometry		
	Standard pin	Tri-flute pin	Cone-shaped pin
300 rpm/2 ipm	x	x	x
700 rpm/8 ipm	x	x	x
900 rpm/8 ipm	x	-	-
1100 rpm/8 ipm	x	-	-

Table 2. Size and aspect ratio of Si particles and porosity volume fraction in FSP and as-cast A356.

Material	Particle size (μm)	Aspect ratio	Cavity volume fraction (%)
Cast	7.28 ± 5.47	3.25 ± 2.51	0.95
FSP-300rpm/2ipm (Standard tool)	2.84 ± 2.37	2.41 ± 1.33	0.11
FSP-700rpm/8ipm (Standard tool)	2.62 ± 2.31	1.93 ± 0.86	0.050
FSP-900rpm/8ipm (Standard tool)	2.55 ± 2.21	2.00 ± 1.01	0.027
FSP-1100rpm/8ipm (Standard tool)	2.51 ± 2.00	2.04 ± 0.91	0.042
FSP-300rpm/2ipm (Tri-flute-pin)	2.70 ± 2.26	2.30 ± 1.15	0.087
FSP-700rpm/8ipm (Tri-flute-pin)	2.50 ± 2.02	1.94 ± 0.88	0.024
FSP-300rpm/2ipm (Cone-shaped-pin)	2.90 ± 2.46	2.50 ± 1.35	0.094
FSP-700rpm/8ipm (Cone-shaped-pin)	2.86 ± 2.32	2.09 ± 0.90	0.032

Table 3. Tensile properties of as-cast and FSP A356 at room temperature.

Materials	As-received or as-FSP			Aging (155^{o}C/4h)		
	UTS, MPa	YS, MPa	El., %	UTS, MPa	YS, MPa	El., %
As-cast	169 ± 10	132 ± 5	3 ± 1	153 ± 7	138 ± 6	2 ± 1
FSP-300rpm/2ipm (Standard pin)	205 ± 6	134 ± 5	31 ± 2	206 ± 6	137 ± 9	29 ± 2
FSP-700rpm/8ipm (Standard pin)	242 ± 6	149 ± 10	31 ± 1	247 ± 7	169 ± 10	28 ± 2
FSP-900rpm/8ipm (Standard pin)	266 ± 4	171 ± 6	32 ± 1	288 ± 5	228 ± 9	25 ± 2
FSP-1100rpm/8ipm (Standard pin)	242 ± 3	157 ± 3	33 ± 1	265 ± 2	205 ± 8	23 ± 5
FSP-300rpm/2ipm (Tri-flute pin)	202 ± 5	137 ± 4	30 ± 1	212 ± 5	153 ± 20	26 ± 3
FSP-700rpm/8ipm (Tri-flute pin)	251 ± 5	171 ± 14	31 ± 1	281 ± 5	209 ± 3	26 ± 2
FSP-300rpm/2ipm (Cone-shaped pin)	178 ± 2	124 ± 5	31 ± 4	175 ± 2	119 ± 6	32 ± 1
FSP-700rpm/8ipm (Cone-shaped pin)	256 ± 5	169 ± 3	28 ± 2	264 ± 4	203 ± 10	21 ± 1

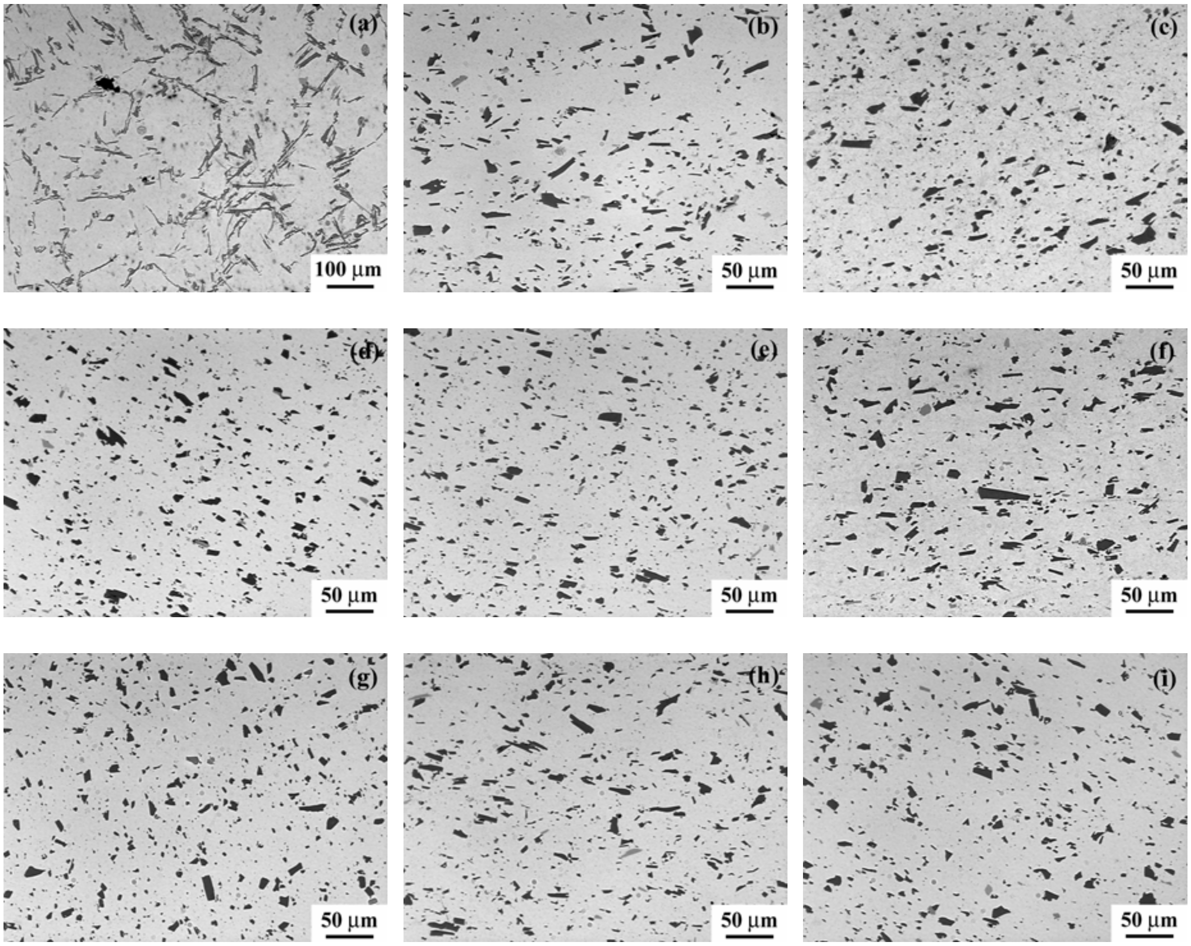

Figure 1 Optical micrographs showing the microstructure of (a) as-cast A356 and (b)-(i) FSP A356: (b) standard pin, 300rpm/2ipm, (c) standard pin, 700rpm/8ipm, (d) standard pin, 900rpm/8ipm, (e) standard pin, 1100rpm/8ipm, (f) tri-flute pin, 300rpm/2ipm, (g) tri-flute pin, 700rpm/8ipm, (h) cone-shaped pin, 300rpm/2ipm, and (i) cone-shaped pin, 700rpm/8ipm.